Electrical Discharge in Deeply Subcritical Field of Microwave Beam in a High-Speed Air Stream and in Propane-Air Mixture

Dmitry V. Bychkov[*], Igor I. Esakov[†], Lev P. Grachev[‡], Kirill V. Khodataev[§]
FSUE "Moscow Radiotechnical Institute of Russian Academy of Sciences", Moscow, Russia

and

David M. Van Wie[**]
The John Hopkins University Applied Physics Laboratory, Laurel, MD, USA

Results are present of an investigation into the characteristics of an electric gas discharge generated in the deeply subcritical field of a quasi-optical microwave (MW) beam. The electrical gas breakdown is initiated by a tubular electromagnetic vibrator. The discharge is realized in a submerged high-speed stream of either air or a propane-air mixture. The stream flows from an internal hole in the aft end of the vibrator, which has sharpened points to serve as initiation sites. A short quartz tube covers the aft end of the vibrator to stabilize the stream. Experiments have been carried out for flow velocities in the range of several hundred meters per second. Photographs of the discharge area have been collected and measurements of the stagnation temperature in the wake of the discharge have been obtained. In this experimental configuration, the experiments show that a MW discharge is realized in the aft area of the vibrator attached to the sharpened ends of the vibrator. This discharge is shown to ignite and stabilize the combustion of a lean propane-air mixture. Complete propane combustion occurs for stream velocities smaller than some threshold value. At larger velocities in the experiments, we have observed effects of thermal choking and throttling of the stream.

I. Introduction

In the present article we describe the results of experiments with deeply subcritical MW discharges in a high-speed stream of either air or a propane-air flammable mixture. These experiments are a continuation of a series of previously reported investigation [1,**Ошибка! Закладка не определена.**].

The discharge is realized in a linearly polarized quasi-optical MW-beam. The magnitude of the ambient electric field component of the electromagnetic (EM) wave, $\boldsymbol{E}$, is substantially smaller than the critical level $\boldsymbol{E}_{cr}$ necessary for a self-maintained electrodeless gas discharge at a given pressure, p. Initiation of a discharge at the experimental conditions requires the use of an EM vibrator, which serves to focus the EM field to a local field strength above $\boldsymbol{E}_{cr}$. This MW discharge "burns" in a high-speed airstream or a flammable mixture made from propane and air. In the later case, local energy addition occurs from both the MW discharge and the combustion processes.

In the reference [1] experimental results are described on the ignition of a propane-air mixture at the aft end of an EM vibrator using a deeply subcritical MW discharge. For these experiments, the vibrator was located in a quasi-optical EM beam parallel to the incident MW vector $\boldsymbol{E}$. Further, the vibrator was located in a submerged high-speed airstream as illustrated in Fig.**1**. The flow velocity v_{fl} was varied from 10 m/s to 500 m/s. In the given scheme, propane was delivered directly to the aft area of the vibrator through internal routing through the vibrator. Propane was injected at the aft end of the vibrator where it mixed air and was subjected to a simultaneous MW discharge. Ignition of both the MW discharge and combustion took place in this area. A photograph illustrating this situation is shown in **Fig.1**, which corresponds to results typical for flow velocities, v_{fl}, in the range of 200 to 500 m/s. Measurements made in the wake region of this discharge have shown that this scheme results in an ignition of the flammable mixture and stabilization of the combustion region; however, the percentage of propane combusted was not very large.

---

[*] Senior engineer, Department of plasma physics
[†] Deputy director on Sci., PhD
[‡] Group manager, Department of plasma physics
[§] Head of plasma physics department, Professor, Dr. of phys.-math. sci., Member AIAA
[**] Principal Professional Staff, Associate Fellow AIAA

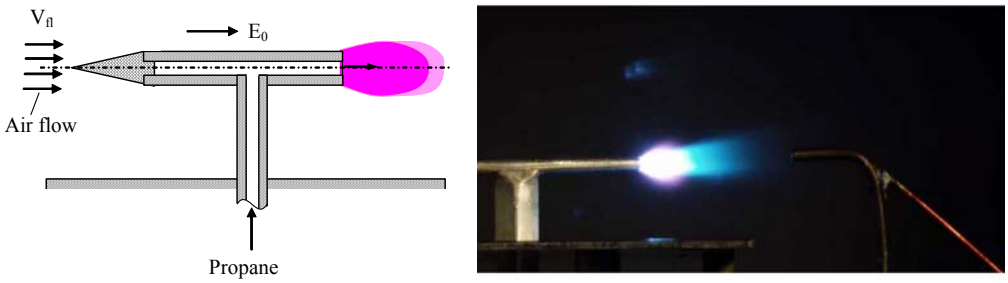

Figure 1. An experiment with propane injection in the aft area of EM vibrator subject to a MW discharge.

In Ref. [2], air was captured at the leading edge of the EM vibrator and internally mixed with propane prior to injection of the fuel-air mixture at the aft end as shown in Fig.**2**. The device was tested in an airstream with v_{fl} = 500 m/s. A deeply subcritical MW discharge was initiated at the aft end of the vibrator. A photograph illustrating this scheme is also shown in Fig.**2**. These experiments showed that complete propane combustion is possible with this configuration. Combustion was also shown to be controllable over a range of fuel-air mixtures.

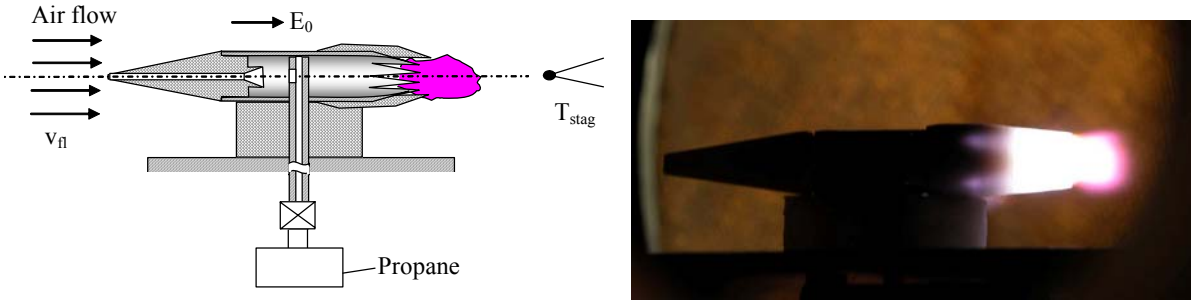

Figure 2. An experiment with propane –air mixture forming in internal region of EM vibrator initiating MW discharge

In Ref. [2] experiments were described on the ignition of a premixed propane-air flow in a submerged airstream using a deeply subcritical MW discharge initiated with an EM vibrator. The results showed that the discharge could ignite such a mixture and stabilize its region of combustion over the range of investigated low velocities. Illustrating photos at v_{fl} = 11 m/s are presented in Fig.**3** corresponding to an approximately stoichiometric composition of the flammable mixture (i.e. fuel-air equivalence ratio $\Phi \approx 1$) and in a lean mixture with $\Phi = 0.24$.

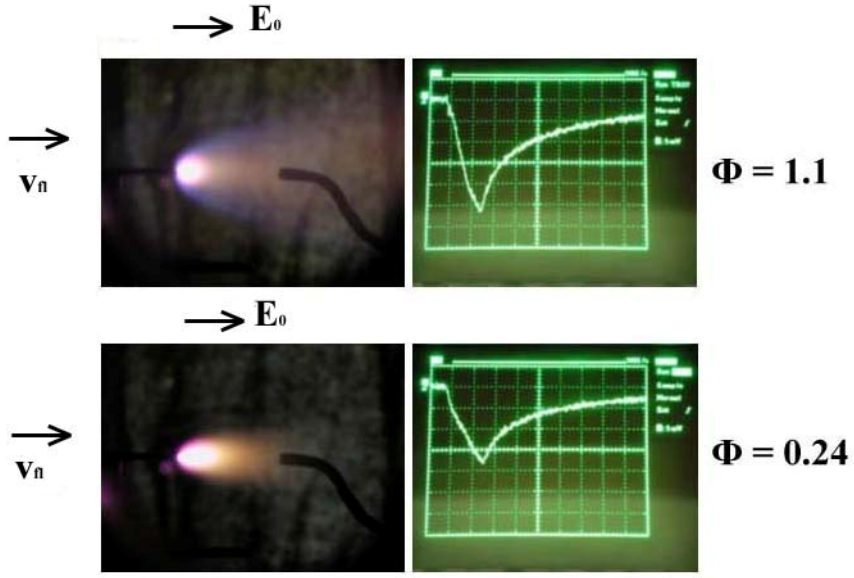

Figure 3. An experiment on ignition of the pre-mixed propane-air flowin a submerged airstream initiated by a MW discharge

In the present work we also describe experiments with a MW-discharge ignited in a quasi-optical EM beam of deeply subcritical field levels. The electrical breakdown is initiated using a tubular EM vibrator through which a high-speed subsonic airflow or a mixture of propane-air is injected.

II. Experimental set up

The scheme of the experimental set up is illustrated in Fig.**4**, and a photograph of its working area is in Fig.**5**. Elements included in the composition of the sheme are designated in the figures using a common numbering scheme.

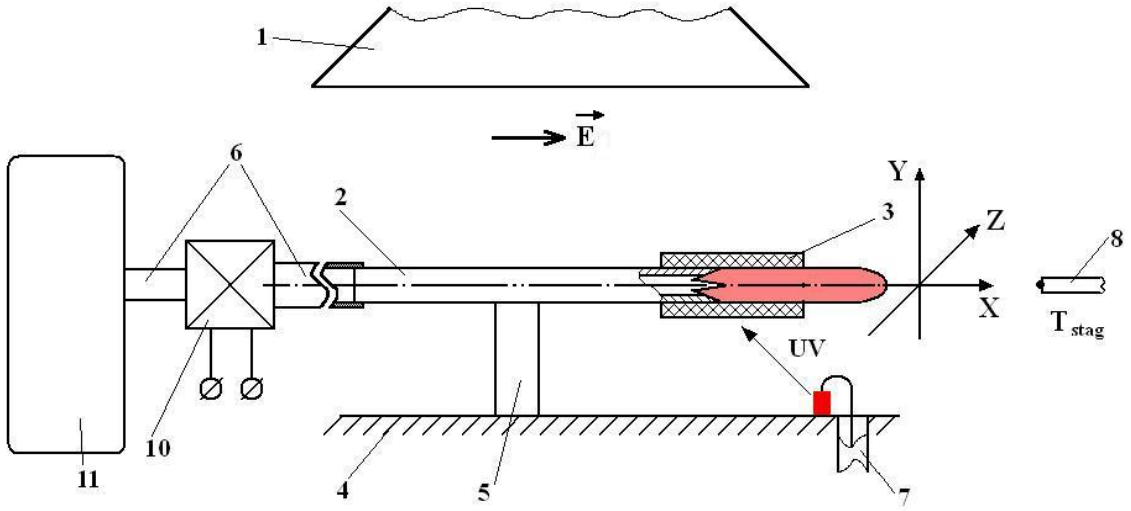

Figure 4. A scheme of the experimental set up

A magnetron MW generator, with output power P_{gen} = 1.5 kW, is used to produce an EM-wave that propagates from the outlet of the generator through a waveguide with an internal cross section 45x90 mm. The waveguide connects to a rectangular horn antenna with 150 mm length and an opening area of 90x90 mm. This arrangement produces a linearly polarized EM-wave with wavelength λ = 12.3 cm in the form of a quasi-optical MW beam that is radiated into the working test chamber. The EM radiation from the horn in Fig.**5** is directed downward, and the vector ***E*** is horizontal.

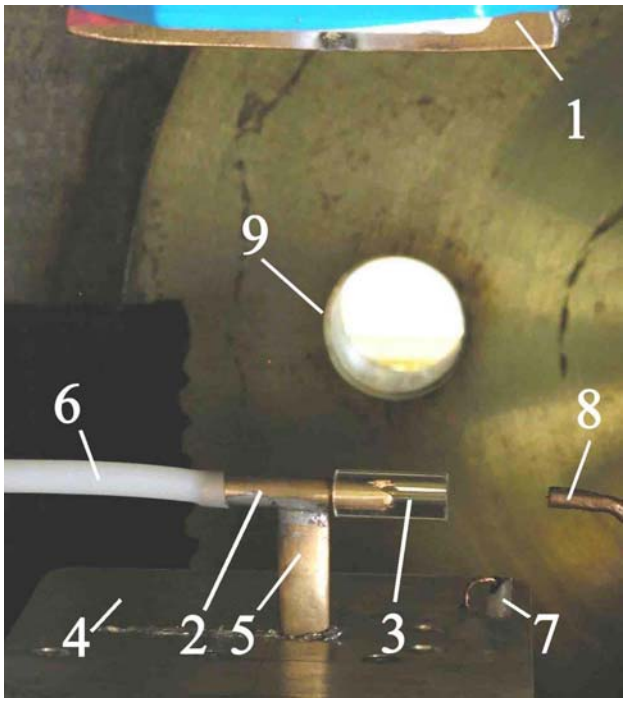

Figure 5. Working area of the experimental set up

A copper tube **2** with external diameter d_{out} = 4 mm and internal diameter d_{in} = 2 mm is located in the MW beam. Its axis is parallel to the vector ***E*** as shown in Fig.**1**, and it stands at a distance of 90 mm from the opening of the radiating horn. The cross-sectional area of the EM beam in the plane of the tube location is approximately equal to

124 cm^2. Thus, the average EM energy flux density of the incident beam in this plane is $\boldsymbol{\Pi} \approx 12$ W/cm^2, which corresponds to a field amplitude $E_0 = 95$ V/cm. One face of the tube is flat (in the photo the flat surface is on the left), and another has three triangular sharpened points. The points, which have a depth of 4 mm, are uniformly space around the periphery of the tube face. One point is oriented towards the Pointing vector $\boldsymbol{\Pi}$ of the EM-beam. The tube – nozzle **3** tightly covers the face of the tube points. Its external diameter is 5.5 mm with a total length of 22 mm and the length of the section downstream of the sharpened ends of the vibrator is $L_{out} = 9$ mm.

The vibrator tube **2** is placed above a metallic plate **4**, which is oriented perpendicular to the vector $\boldsymbol{\Pi}$. The distance from the tube axis to the plate surface is $h = 30$ mm and is located in the EM-field at a position where the local ambient electric field is $\boldsymbol{2E_0}$. Note that the induced current in the metallic vibrator is equal to zero in the central part of the tube when its length is $\mathbf{2L} \lesssim \boldsymbol{\lambda/2}$. This allows the tube to be fixed to the bar **5** and then fastened to the plate **4** without generating a shorting current. The bar length is 10 mm along the tube axis with a 2 mm thickness.

A polyethylene tube **6** (with internal diameter of 4 mm and wall thickness of 1 mm) is attached to the flat end of the tube-vibrator and overlaps for a length of 6 mm. An electrically controlled valve **10** (with conditioned thru-diameter equal to 10 mm) is included. The tube **6** is connected to a pressure vessel **11** with a volume $V_b = 5.2 \cdot 10^3$ cm^3. Pressure in this vessel can be established in the range $p_b = (760 - 0.1)$ Torr.

In Fig.**5** one can see a device for producing ultra-violet (UV) radiation **7** on the right side of the plate **4**. Its purpose will be explained below.

The vibrator is located in a test chamber of volume 4.5 m^3. The air pressure $\boldsymbol{p_c}$ in it can be established in the range from 760 to 3 Torr. The chamber has windows through which optical recording of investigated processes takes place. One of windows is seen in Fig.**5** and is designated by the number **9**.

At $\mathbf{p_c < p_b}$ gas from the pressure vessel starts to flow into the test chamber when valve **10** is opened and a flow stream is formed at the outlet of the quartz tube **3**.

Stagnation temperature $\boldsymbol{T_{stag}}$ downstream of the vibrator is measured using a thermocouple **8**. To prevent MW noise, the wires leading from the "hot" joint of the thermocouple are routed through a metallic screening tube (with an external diameter of 4 mm). The thermocouple junction stands out from the screen face 1mm. The sensor **8** is located along the axis of the flow with the thermocouple joint located at a distance $x = 40$ mm from the end of the quartz nozzle **3**. For steady state operation, the average sensitivity of the applied sensor is $S_T = 24.5$ °K/mV for temperatures up to 1100 °C. The key time-dependent features of the $\boldsymbol{T_{stag}}$ measurement using this sensor will be described below.

III. Resonance features of the tube EM vibrator

The resonance length $2L_{res}$ of an EM vibrator depends substantially on its design parameters. Using a vibrator with length $2L_{rez}$, the field is maximal at its ends but no current is induced in it. In the present work, the main investigations were conducted using a length $2L_{rez}$ for the tube vibrator with the quartz nozzle applied to its end.

Initial experiments were conducted with the vibrator placed over the plate at a height h on a foam plastic support rather than being firmly fixed to the screen using a metallic bar. In experiments carried out without flow, the maximum air pressure p_{br} was determined for which the vibrator still initiated electrical air breakdown. The experiments began with a maximum tube 2 length of $2L = 53$mm. The length $2L$ was then gradually decreased by cutting from the flat end of the vibrator. The existence of the breakdown in the experiments was detected using the visual emission from the MW discharge in areas near the end of the vibrator.

The main experiments were undertaken using a MW pulse width of $\tau_{MW} \approx 0.2$ s. However, initial experiments showed that air breakdown was not repeatable for this $\boldsymbol{\tau_{MW}}$ in successive MW pulses conducted at constant conditions. This lack of repeatability, especially at an air pressure p on slightly lower than p_{br}, can be explained by the small volume of the region where the induced field $\boldsymbol{E > E_{cr}}$ and the likely absence of free electrons in this volume during $\boldsymbol{\tau_{MW}}$. These free electrons are necessary for initiation of the breakdown avalanche development, so no discharge will occur without their presence.

To enable repeatable results, a source of UV radiation **7** was incoporated into the experimental scheme, see **Fig.4** and **Fig.5**. This radiation is generated by a spark discharge between the core of a high voltage (HV) cable and the surface of the plate ***4***. The HV pulse is delivered to the cable simultaneously with the corresponding initiation of the HV feed to the MW generator. The experiments showed that the irradiation of the tube **2** end with UV radiation results in repeatable MW breakdown in the presence of the quartz nozzle **3**. This discharge develops near this end of the vibrator inside the quartz nozzle.

In **Fig.6** for reference we present a design for the EM vibrator and a graph of the $p_{br}(2L)$ dependence based on the experimental results. From the results, it is follows that the length is $2L_{rez} \approx 48$ mm, which is 13.5 mm smaller than the size $\lambda/2 = 61.5$ mm. The vibrator in this configuration ensures air breakdown for pressures up to $p_{br} \approx 280$ Torr, corresponding to a Q-factor of $Q \approx 5.5$. For the main experiments, which were conducted at $p_c = 120$ Torr, a vibrator with $2L = 47$ mm was used.

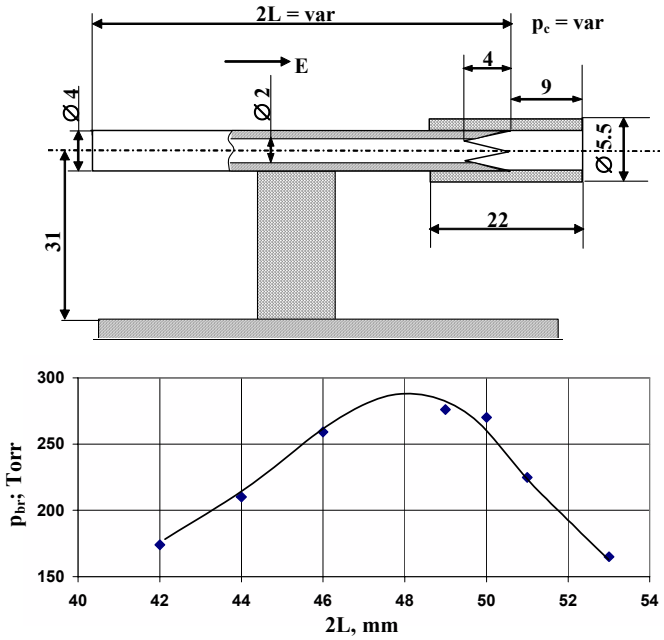

Fig. 6. Resonant features of the tubular linear EM vibrator with quartz nozzle

IV. Parameters of the submerged air stream

In the experiments we aimed to produce the discharge in the high-speed subsonic air stream that which is generated for pressure ratios $1 < (p_b / p_c) < 1.9$. With a goal of operating within this range, the initial pressure p_b was set to 200 Torr for experiments conducted at $p_c = 120$ Torr.

In the experiments the signal for the valve **10** opening in the duct of the stream formation had a duration of 0.7 s. Control measurements showed that the time of steady air outflow from the pressure vessel was $\tau_{fl} = 0.66$ s for these condiitons. The pressure p_b during the time τ_{fl} dropped by some value Δp_b , which was measured in the experiment. During this τ_{fl} the MW generator was switched on for $\tau_{MW} = 0.2$ s, and the signal from the T_{stag} sensor was detected using an oscilloscope. Then the whole cycle was repeated but at a lower initial pressure in the pressure vessel. The number of cycles within a test series is designated by the index K. Experimental series were conducted with K as large as $K = 10$. In Fig.**7** the experimentally measured Δp_b is shown as a function of K, as obtained during several experimental series. A common symbol is used for all data points from the same series (and the same configuration). The trend of Δp_b (K) is given by the solid line.

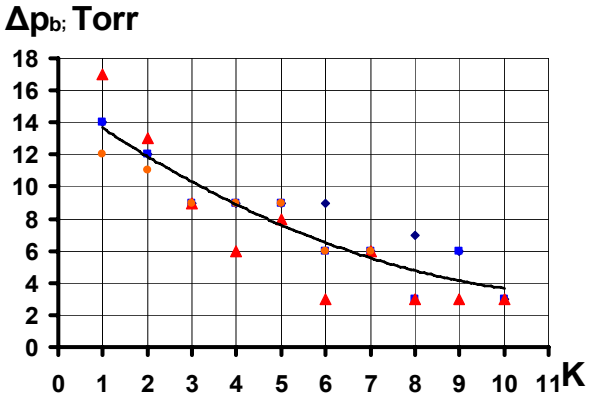

Figure 7. Experimental pressure drop Δp_b in the balloon in each succession cycle K of air outflow

In Fig.**8** the initial pressure in the pressure vessel p_b is shown as a function of K after accounting for the experimentally measured Δp_b. One can see in Fig.**8** that p_b drops from the initial value of 200 Torr almost to the chamber pressure p_c (120 Torr) by the tenth cycle. As p_b approaches p_c, the value of Δp_b is not repeatable in different series due to the design of the test apparatus. Thus, no correct quantitative conclusions can be developed for experiments with cycle numbers $K \geq 10$. The ratio of pressures p_c and p_b allows one to calculate the Mach number M of the formed air stream for each K:

$$M = \sqrt{5 \cdot \left(\frac{1}{(p_c / p_b)^{1/3.5}} - 1 \right)}. \qquad (1)$$

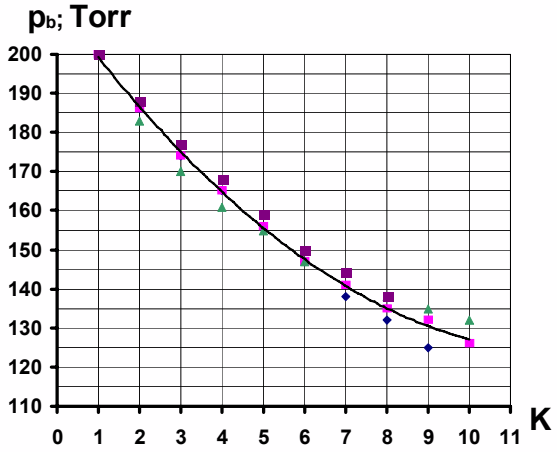

Figure 8. Pressure in supply vessel p_b before beginning of each successive cycle *K* of air outflow

The Mach numbers *M* calculated using this formula and an approximating curve are presented in Fig.**9.** It follows from thse results that the Mach number in the experimental series decreases nearly linearly from $M \approx 0.9$ to $M \approx 0.3$ for cycles between 1 and 10.

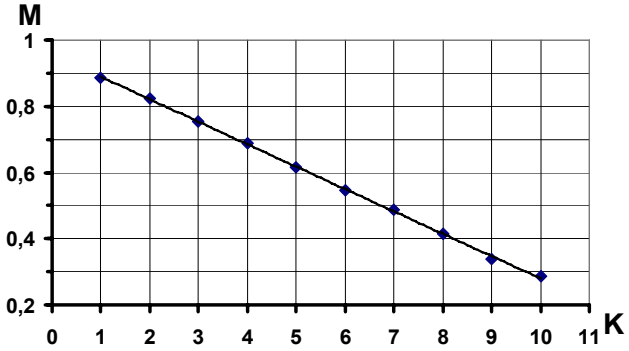

Figure 9. Mach number *M* of the flow at the outlet of air outflow duct foreach cycle *K*

Knowing *M*, the flow velocity at the outlet from the duct is estimated from:

$$\mathrm{v_{fl}} = 340 \cdot M / (1 + 0.2 \cdot M^2)^{0.5}, \text{ m/s.} \qquad \textbf{(2)}$$

Values of v_{fl} calculated using (2) are presented in Fig.**10**.

Using the measured drop in air pressure Δp_b during each cycle *K* during the time τ_{fl}, the mass flow rate can be estimated as:

$$m_{air} = \frac{\mathrm{V}_b}{\tau_{fl}} \cdot \rho_0 \cdot \frac{\Delta p_b}{760}, \text{ g/s.} \qquad (3)$$

In this formula, Δp_b - Torr, V_b – cm^3, τ_{fl} – s and $\rho_0 = 1.23 \cdot 10^{-3}$ g/cm^3 is the air density at standard conditions. The calculated m_{air} values for different *K* are shown with the solid line in Fig.**11**.

The air mass flow rate can be also calculated using the expected outlet parameters of the stream:

$$m_{air} = \rho_{out} \cdot \mathrm{v_{fl}} \cdot S_{out} \equiv \rho_0 \cdot \frac{p_b}{750} \cdot \frac{1}{\left(1 + 0.2 \cdot M^2\right)^{2.5}} \cdot 3.4 \cdot 10^4 \cdot \frac{M}{\left(1 + 0.2 \cdot M^2\right)^{0.5}} \cdot \frac{\pi \cdot d_{in}^2}{4}, \text{ g/s.} \qquad (4)$$

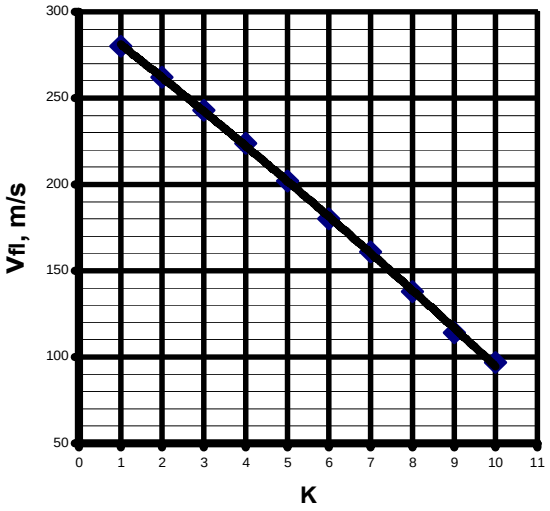

Figure 10. The flow velocity v_{fl} at the exit from the outflow duct in each cycle *K*

In this formula values of p_b for each K are taken from the graph in Fig.**8** and Mach numbers, M, from the graph in Fig.**9**. The outlet diameter is taken to be $d_{in} = 0.2$ cm. The calculated values of $\boldsymbol{m_{air}}$ using this approach are also shown in Fig.**11** and are connected by the dashed line. One can see that this line lies up to a maximum 30% higher than that calculated using formula (3). This agreement gives grounds for the of the $M(K)$ and $v_{fl}(K)$**,** which have been obtained by formulas that assume one-dimensional steady adiabatic flow of an ideal gas through a tube with varying cross section area.

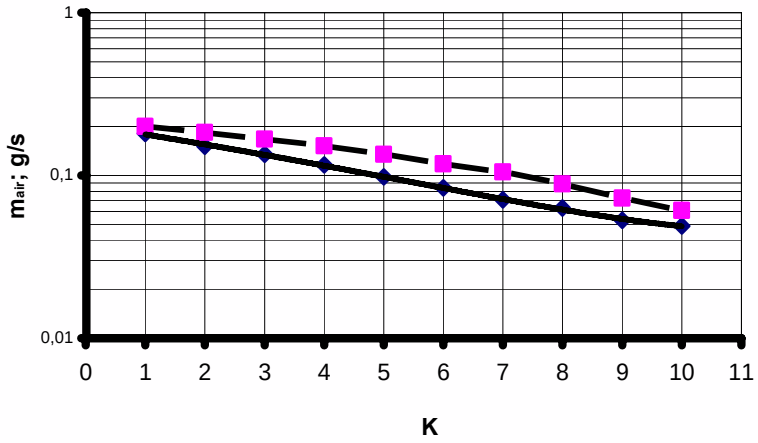

Figure 11. Mass flow rate of air $\boldsymbol{m_{air}}$ (solid line) from the balloon of its outflow and at outlet of the outflow duct (dashed line) in each cycle *K*

V. Deeply subcritical MW-discharge in the high-speed air stream

The experimental results have shown that a MW discharge was initiated in the aft area of the EM vibrator over the entire range of flow velocities v_{fl} for this experimental setup, but the appearance of the discharge depends on v_{fl} . In Fig.**12** a typical time integrated photograph of the discharge is shown for a comparably high $v_{fl} = 240$ m/s (corresponding to $K = 3$), which can be contrasted to that shown in Fig.13 that was obtained at a comparably low $v_{fl} = 160$ m/s (corresponding to $K = 7$).

In the photos one can see the aft end of the vibrator with the quartz nozzle and the downstream thermocouple, which is used to measure T_{stag}. It follows from the photos that the discharge partially burns inside the quartz nozzle touching the sharpened ends of EM vibrator and partially downstream in the flow emitting from the nozzle. The symmetry along the axis of the system vibrator-nozzle downstream of the nozzle depends on the flow velocity v_{fl}.

Figure 12. Deeply subcritical initiated MW discharge in air submerged MW stream at comparably high flow velocity

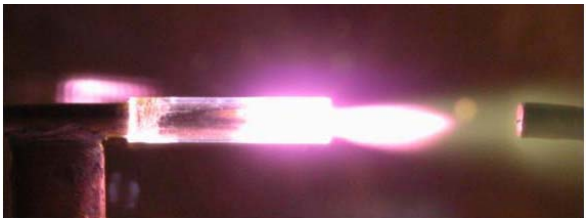

Figure 13. Deeply subcritical initiated MW discharge in air submerged MW stream at comparably low flow velocity

The discharge area at large v_{fl} is shifted upward with respect to the axis as seen in Fig.**12**. The length of the luminescence area L_{dis} as measured from the aft end of the nozzle is approximately equal to 15 mm, i.e. the total length of the discharge area is $(L_{out} + L_{dis}) \approx 24$ mm. The maximum transverse size of this area is $d_{dis} \approx 9.5$ mm. One can see in the photograph that the luminescence in the area of vibrator's sharpened end is so intense that it creates a "spherical" halo outside the quartz nozzle, and a comparably long trail glowing whitish color is located downstream in the flow behind the discharge area. One can postulate that this is the result of the chemo luminescence of molecules excited in the discharge.

The discharge burns relatively symmetrically about the system axis at small v_{fl}, as seen in Fig.**13**. Its length is $L_{dis} \approx 20$ mm and the diameter is $d_{dis} \approx 11$ mm. These dimensions are somewhat larger than the corresponding size of the discharge presented in Fig.**12**. The "whitish" trail is also wider.

In Fig.**14** the waveforms obtained from the thermocouple are presented with the waveforms identified using their number K in a cycle. The vertical scale in the figure is 5 mV/div, and the horizontal scale is 0.2 s/div. The waveforms show that the T_{stag} measurements do not reach steady state, so the inertial response of the thermocouple must be considered. The start of the thermocouple signal growth corresponds to the moment of MW discharge ignition and the maximum $\boldsymbol{U_m}$ to the beginning of its decay. Thus, the actual discharge time is $\tau_{dis} = 0.18$ s. The decreasing portion of the waveform corresponds to the cooling of the thermocouple junction.

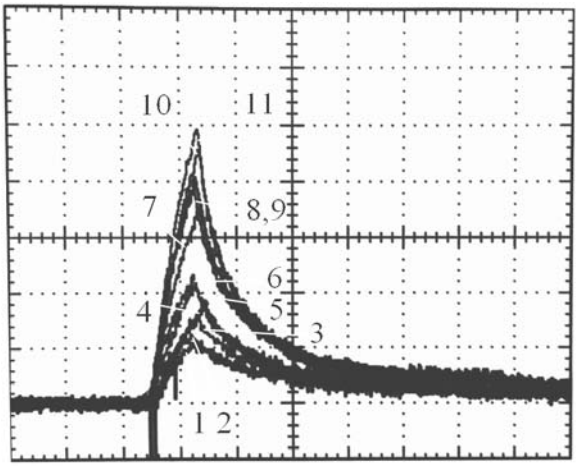

Figure 14. A signal from the thermocouple T_{stag}measurer in the successive cycles K of air outflow at burning MW discharge in it

Assuming that the readings of the T_{stag} sensor vary in time t due to a step change in flow temperature according to:

$$U = U_0 \cdot (1 - e^{-t/\tau}), \tag{5}$$

where the time constant $\boldsymbol{\tau}$ characterizes the inertia of the sensor, and $\boldsymbol{U_0}$ represents the steady-state value corresponding to T_{stag}. From the waveforms shown in Fig.**14,** it is estimated that $\tau = 2.2$ s. Using this $\boldsymbol{\tau}$ value together

with the discharge time, τ_{dis} and the sensor sensitivity S_T, the stagnation temperature rise in the flow following the MW discharge can be calculated from:

$$\Delta T_{dis} = 1.8 \cdot U_m \cdot S_T \text{, K.} \tag{6}$$

Values of ΔT_{dis} calculated with the help of Fig.**14** for each K are shown in Fig.**15** and are approximated by two solid lines. The results show that ΔT_{dis} rises from 200 °K to 1100 °K with increasing K and corresponding decreasing v_{fl}. Note that the dependence $\Delta T_{dis}(K)$ has a "break" in the region of K = (5 - 7), which will be discuss later.

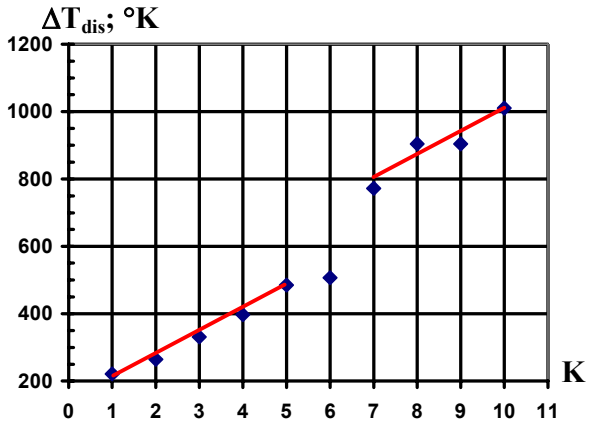

Figure 15. ΔT_{dis} gas temperature rise in the result of MW discharge ignition in air stream in the successive cycles K of the scheme switch on

In the experiments, the appearance of the discharge for $K \leq 5$ is similar to that shown in Fig.**12**, and at $K \geq 7$ to that in Fig.**13.** At K = 6 the discharge appearance varied from test to test in successive series. At this value of K only a bright luminescence is recorded in the area surrounding the quartz nozzle.

Using the experimentally measured ΔT_{dis} and air mass flow rate values m_{air}, the discharge power P_{dis} heating the air is estimated from:

$$P_{dis} = c_p \cdot m_{air} \cdot \Delta T_{dis} \tag{7}$$

where c_p = 1 J/(g·°K) is assumed. P_{dis} is nearly constant for K = (7 - 10) at a level of $P_{dis} \approx 60$ W. Using the known energy flux density Π in the area of EM vibrator location, this value of P_{dis} gives the effective area of energy thermal interaction with the system EM vibrator- discharge plasma – $S_{eff} = P_{dis} / \Pi \approx 5$ cm^2 . This area is approximately 7 times greater than the longitudinal discharge cross section area, which can be estimated from the photograph in Fig.**13** to be $S_{dis} \approx 0.7$ cm^2.

VI. Deeply subcritical MW-discharge in a high-speed of propane-air mixture

Microwave discharges in a combustible medium were investigated using a mixture of propane-air. In preparing the experiments, the pressure vessel initially was pumped down to $p_b \approx 10^{-1}$ Torr, and then filled with propane (C_3H_8) to a specified pressure $p_{C_3H_8}$. Next, the pressure vessel was filled with air up to atmospheric pressure p_Σ. Finally, the homogeneous propane-air mixture was pumped down to p_b = 200 Torr. From this initial p_b value, the experiments were initiated and and the experimental cycles K were executed at a constant p_c = 120 Torr.

It is known that the normal range for propane-air ignition lies between Φ = (0.6 - 2.7). For the initial experiments, $p_{C_3H_8}$ = 21 Torr was set, which corresponds to Φ = 0.8 (i.e., a lean but flammable mixture). A photograph showing the discharge for K = 1 is shown in Fig.**16.** The principal appearance of the combustion area changes only weakly with increasing K**.** The maximum level of the signal U_m from the thermocouple for all K was substantially smaller than that obtained from the MW discharge in pure air. In addition, the form of the signal weakly corresponded to the law with exponential saturation.

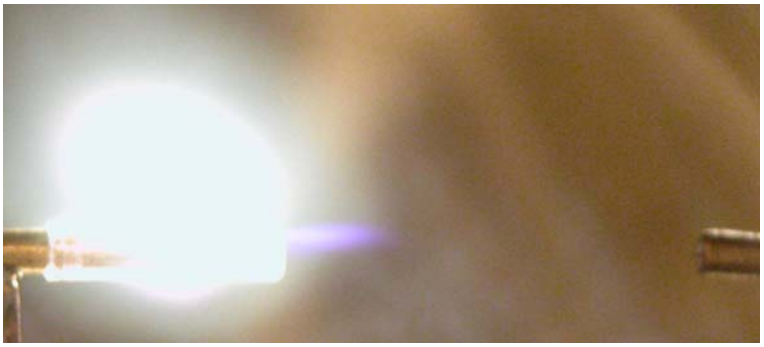

Figure 16. ***MW discharge in propane-air stream at fuel excess coefficient Φ = 0.8.***

One can propose that a thermal choking of the outflow duct takes place in the given experimental conditions, which is caused by the substantial heat release within the quartz tube [3]. In attempting to minimize the effect of this thermal choking, the main series of experiments were conducted using $p_{C_3H_8} = 3$ Torr, which corresponds to $\Phi = 0.11$. This mixture is leaner that the normal range of propane-air flammability. The appearance of the discharge zone in these experiments for different K were nearly identical with those conducted in pure air which were shown in Figs. 12 and 13, but the thermocouple readings indicated a larger level for U_m . The corresponding waveforms for various K are presented in Fig.**17**.

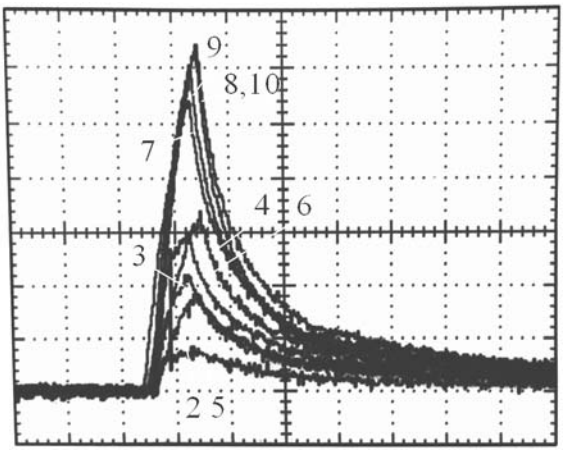

Figure 17. ***A signal from the thermocouple measurer of T_{stag} in the successive K cycles of propane-air mixture outflow at MW-discharge burning in it***

Values for ΔT_{mix} calculated from Fig.**17** with application of fomula (6) are shown in Fig.**18** connected by approximating lines. Overlaid on this figure are the results from Fig.**15** corresponding to the discharge in pure air. Comparison of results shows that the temperature of the gas that passed through the discharge area increases when propane is present in the flow; hence, propane-air mixture combusts in the presence of the discharge.

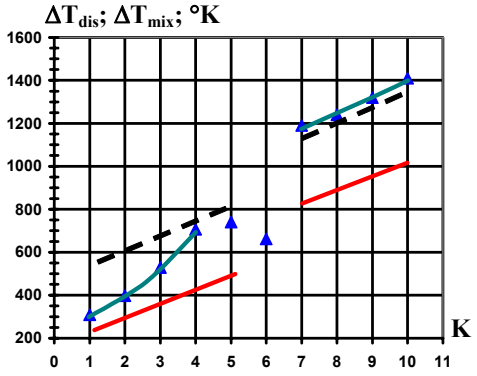

Figure 18. Gas temperature rise ΔT_{mix} in the result of MW discharge realization in the stream of propane-air mixture in the successive *K* cycles of the scheme switch on

In Fig.**18** two additional dashed lines are included corresponding to complete propane combustion in the mixture. These values were calculated as follows. The power of propane combustion is

$$P_{com} = m_{C_3H_8} \cdot \mathrm{Q}_{com}\ ;\ \mathrm{W}, \tag{8}$$

where $m_{C_3H_8}$ is mass flow rate of propane in g/s, and $\mathrm{Q}_{com} = 4.64 \cdot 10^4$ J/g is the specific energy of its combustion. The value for $m_{C_3H_8}$ can be estimated as:

$$m_{C_3H_8} = m_{air} \cdot \frac{p_{C_3H_8}}{p_\Sigma - p_{C_3H_8}} \cdot \frac{\rho_{C_3H_8}}{\rho_{air}}\ ;\ \mathrm{g/s}, \tag{9}$$

where $\rho_{C_3H_8} = 2.2 \cdot 10^{-3}$ g/cm^3 is the propane density at standard conditions. Calculated values for $m_{C_3H_8}$ give the propane mass flow rate for different K in the range from $1.4 \cdot 10^{-2}$ g/s to $3.6 \cdot 10^{-4}$ g/s. Combining formula (7) with corresponding change of indexes and formulas (8) and (9), the following equation is obtained for additional air heating as a result of propane combustion:

$$\Delta T_{C_3H_8} = \frac{1}{c_p} \cdot \frac{p_{C_3H_8}}{p_\Sigma - p_{C_3H_8}} \cdot \frac{\rho_{C_3H_8}}{\rho_{air}} \cdot \mathrm{Q}_{com}\ ;\ ^\circ\mathrm{K}. \tag{10}$$

Inserting the corresponding values into this formula, one gets $\Delta T_{C_3H_8} \approx 330$ °K. This value does not depend on the cycle number K, because the ratio $m_{C_3H_8} / m_{air}$ is constant. In Fig.**18** the dashed lines are presented as an offset to ΔT_{mix} from the MW discharge heating as represented by the solid lines.

A comparison of experimental values of ΔT_{mix} in Fig.**18** with the dashed line leads to the following conclusions. Propane does not completely combust at $K < 4$ which corresponds to velocities grater that $v_{fl} > 220$ m/s. The percentage of combustion increases with decreasing $\mathbf{v}_{fl}$, and the propane combustion can be considered nearly completely at $K \approx 4$, which corresponds to $v_{\mathrm{fl}} \approx 220$ m/s for these experiments. For $K > 7$, the propane combustion is complete as it flows through the MW discharge area.

Next, consider the experimental peculiarity that was observed at $K = 5$ - 6. In reference [3] one-dimensional flow in a tube with heat delivery was studied. The dimensionless Damkohler number was introduced:

$$D = q/(c_p \cdot T_1) \equiv \Delta T_{stag} / T_1\,, \tag{11}$$

where q is amount of thermal energy delivered to a unit of a gas mass, T_1 is its intial temperature, and ΔT_{stag} is this increase in stagnation temperature of the flow with heat addition. In our case: $T_1 = T_0 / (1 + 0.2 \cdot M^2) \approx \mathrm{T}_0$, and ΔT_{stag} is ΔT_{dis} or ΔT_{mix}.

Analysis presented in [3] showed that there is a critical Damkohler number

$$D_{cr} = \frac{1}{2 \cdot (\gamma + 1)} \cdot \left(\frac{1 - M_1^2}{M_1} \right)^2, \tag{12}$$

where the adiabatic exponent for air is $\gamma = 1.4$ and M_1 is the Mach number of the flow approaching the area of heat delivery. A steady state of the flow can not be realized for $D \geq D_{\mathrm{cr}}$ due to thermal choking. It follows from (12) that the number D_{cr} approaches zero as M_1 approaches 1, and at $M_1 = 1$ it is impossible to deliver heat to a steady flow in the tube.

For example, in the described experiments the initial Mach number is $M = 0.55$ at $K = 6$ and according to (12) $D_{\mathrm{cr}} = 0.335$. One can propose that the peculiarity observed in the experiments at $K = (5 - 6)$ is caused by the equality $\mathrm{D} \approx \mathrm{Dcr}$. Let us suppose that all the molecules were heated up to $\Delta T_{\mathrm{dis}} \cdot \xi$ in the internal region of the quartz nozzle (where the coefficient $\xi < 1$ represents the portion of heat added in this part of the discharge). According to (11), $D = D_{\mathrm{cr}}$ with $\Delta T_{\mathrm{dis}} \approx 600$ °K resulting in $\xi \approx 0.18$ assuming that the energy addition is homogeneous over the discharge volume. From the experiments one can estimate the ratio of the discharge volume within the quartz tube to its entire volume to be about 0.2, which is close to the estimated value of ξ.

There is one additional peculiarity in the experiments. The photographs show a flow throttling at $K = (1 - 4)$ as indicated by the flow nonuniformity in the direction perpendicular to its velocity (see Fig.12). The “steps” in

dependencies of ΔT_{dis} (K) and ΔT_{mix} (K) in different ranges of K in **Figs**. **17** and **18** are connected with this. One can propose that in this experimental formulation the throttling phenomenon takes place at $D > D_{cr}$, and at $D \approx D_{cr}$ we observe an unstable process for which the existence of the throttling that is dependent on small variations of the stream parameters.

VII. Conclusions

As the result of the undertaken MW discharge investigastions, the resonant features of the tubular linear EM-vibrator have been determined with respect to its length $2L \leq (\lambda/2)$ for a specific diameter and geometric construction. The experiments revealed that the maximum induced fields at the ends of the vibrator were reached at a $\boldsymbol{2L_{rez}}$ that is much smaller than $\boldsymbol{\lambda/2}$.

In the experiments a MW discharge was realized in the linearly polarized deeply subcritical feald of the quasi-optical EM beam in airflow at a pressure p_c = 120 Torr and flow velocity $\mathbf{v}_{fl}$ in the range from 280 m/s to 100 m/s. The effective area $\boldsymbol{S_{eff}}$ of energy interaction of a deeply subcritical MW discharge initiated by the linear EM vibrator with MW EM field exciting it was estimated. These results show that this area $\boldsymbol{S_{eff}}$ is substantially greater than the longitudinal cross section of the discharge area $\boldsymbol{S_{dis}}$.

The experiments have shown that such a discharge is capable of igniting propane-air flammable mixtures that propagate through the discharge even when the equivalence ratio Φ is 5 times lower than its normal flammability limit. At these condictions, the propane was shown to combust completely for flow velocities lower than about 200m/s. At higher velocities, the percentage of combustion decreases.

The experiments have shown that in applying this scheme one has to account for the effects of thermal choking and the stream throttling. These features require additional investigation.

Acknowledgement

The work is performed with financial support of EOARD (Project ISTC # 3572p). Authors sincerely thank Dr. Julian Tishkoff for his displayed interest and fruitful discussions.

References

[1] Igor I.Esakov, Lev P.Grachev, Kirill V. Khodataev, D.M.Van Wie *Efficiency of microwave discharges for propane ignition in cold high-speed airflows*, 43rd AIAA Aerospace Sciences Meeting and Exhibit (10-13 January 2005, Reno, Nevada), AIAA 2005-989.

[2] I.Esakov, L.Grachev, K.Khodataev, V.Vinogradov and D.Van Wie *Deeply Subcritical MW Discharge in the Submerged Stream of Propane-Air Mixture*, 46rd AIAA Aerospace Sciences Meeting and Exhibit, Reno, Nevada, 7-10 Jan. 2008, AIAA 2008-1403.

[3] Bartlma F. Combustion Gasdynamics. Moscow. Energoizdat Publ. 1981.